Lawrence Berkeley Laboratory
UNIVERSITY OF CALIFORNIA

Materials & Molecular Research Division

Submitted for presentation at the National Association of Corrosion Engineers Conference, Corrosion '81, Toronto, Ontario, Canada, April 6-10, 1981

CORROSION OF METALS IN OIL SHALE ENVIRONMENTS

A. Levy and R. Bellman, Jr.

December 1980

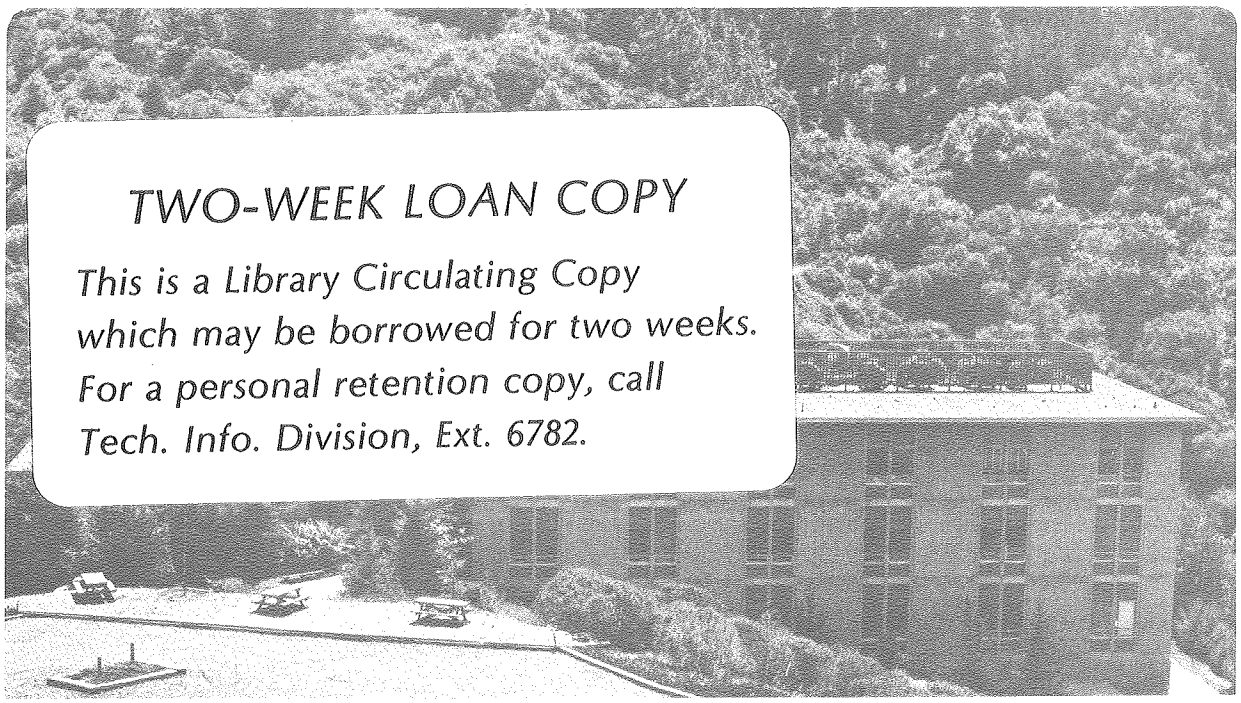

Prepared for the U.S. Department of Energy under Contract W-7405-ENG-48

DISCLAIMER

LBL-12019

CORROSION OF METALS IN OIL SHALE ENVIRONMENTS

A. Levy and R. Bellman, Jr.

Lawrence Berkeley Laboratory
University of California
Berkeley, California 94720

This work supported by the Office of Advanced Research and Technology,
Office of Fossil Energy, U. S. Department of Energy under
Contract No. W-7405-ENG-48

CORROSION OF METALS IN OIL SHALE ENVIRONMENTS

A. LEVY AND R. BELLMAN, JR.

Lawrence Berkeley Laboratory
University of California
Berkeley, California 94720

ABSTRACT

The corrosion of mild, low alloy and stainless steel in elevated temperature in-situ oil shale retorting environments is being investigated. The catastrophic oxidation-sulfidation attack that can occur in in-situ retorts is documented for a thermowell consisting of a mild steel pipe protecting a stainless steel sheathed thermocouple assembly. The behavior of metals under a number of varying conditions such as service temperature, type of shale and oil content of shale is presented. The potential of coatings on mild steel to extend its service range into shale retorting environments has been determined for pack aluminide type coatings.

INTRODUCTION

The corrosion of metal components in the operating environments of in-situ oil shale retorts is being studied in a DOE-FE sponsored program. To date specimens have been analyzed metallurgically using optical microscopes, SEM with EDAX and X-ray diffraction after exposure in 13 above ground, simulated in-situ retorts tests and 1 underground in-situ retort operation. In all cases, corrosion ranging from mild at temperatures near 550°C to severe at temperatures near 1100°C had occurred on both mild and stainless steel specimens and components. (1022-2012°F)

Reference 1 contains a brief description of the in-situ retorting process which utilizes a moving combustion process in the shale body to generate sufficient heat to pyrolize the organic material, kerogen, in the marlstone rock and drive liquid and gaseous products ahead of it to collection sumps where it is drawn to the surface. The high temperatures in the combustion zone and the slowly cooling region behind it coupled with significant quantities of oxygen and sulfur in the retort environment cause oxidation and sulfidation to occur in the metal piping components that extend into and through the hot region.

Variations in the composition of the marlstone oil shale rock and the retorting conditions can result in major differences in the corrosion behavior of mild and stainless steels. Such variables as combustion temperature-time cycles, sulfur content of the shale, and shale oil content of the rock can result in major differences in the severity of the corrosive attack. However, if operating temperatures approach 1100°C for even a few hours, both types of steel are severely attacked. At more mild temperatures near or below 825°C, (1500°F) the difference in the degrees of attack between mild steel and 300 series stainless steels is significant. The Cr_2O_3 protective scale on the stainless steels markedly reduces the amount of corrosion that occurs.

An example of severe attack of a black iron (mild steel) thermowell casing and its 304SS thermocouple sheath is described in the first section of this report. In the second section, the effects of variations in retort operating conditions on corrosion of steel specimens placed in above ground, simulated retorts are discussed. The promising potential of aluminide coatings on steels is presented in the third section of the report.

THERMOWELL PERFORMANCE ANALYSIS

Two badly corroded thermocouple well casings were received for failure analysis. These casings had been removed from an underground in-situ oil shale retort operated by Geokinetics, Inc.

The well casings were originally 3/4-inch black iron pipe (mild steel) and one of the casings still had a thermocouple sheath of austenitic stainless steel and its thermocouple attached to its inside wall. Each casing had been exposed to a retorting environment which produced temperatures of from 550°C to 1100°C. The length of the exposure time was not provided nor was the composition of the retorting gases, but conditions were severe enough to completely deteriorate the casings. Figure 1 shows the two casings.

Optical Microscope Analysis

Specimen B shows heavy scale development on either side of the metal matrix (Fig. 2A). Note the extent of the corrosion and the layered nature of the scale. At its thickest portion, there is but 0.7 mm of casing left. There appear to be some metal islands in the scale on the inside edge (Fig. 2C), while none are seen on the outside edge (Fig. 2B).

Specimen A had been too heavily attacked to permit a useful optical examination to be performed. The casing was so badly corroded that no unattacked metal remained, only scale products. Specimen A did have a fairly intact thermocouple that was removed and photographed (see Fig. 3). A heavy scale is, of course, present but there is also considerable selective attack along the grain boundaries that extends throughout the sheathing. The sensing wires appear undamaged, probably due to the protective ceramic casing.

Electron Microscope Analysis

Initially, a low magnification micrograph of the mild steel casing of Specimen B was taken to show the thicker, layered interior surface scale and the thinner exterior surface scale (see Fig. 4). Also visible is a thin layer of internal sulfidation on either side of the metal matrix. No grain boundary attack is observed. Each primary scale layer on either side of the remaining metal shows only iron present. No sulfur is detected so this is an indirect confirmation of the presence of iron oxide, Fe_2O_3 or Fe_3O_4. Fe_2O_3 was later verified by x-ray diffraction techniques.

The scale layers immediately next to the base metal were examined at a higher magnification and show significant quantities of sulfur as well as iron (see Fig. 5). This confirms the presence of iron sulfide ($Fe_{1-x}S$), (FeS_2), or iron sulfate ($FeSo_4$), depending on retorting conditions such as temperature and the gas partial pressures of sulfur and oxygen.

To more clearly identify this sulfide layer, a high magnification micrograph of the area was obtained. EDAX of various sections show the presence of iron and sulfur (see Fig. 6). EDAX of the round inclusions in the base metal indicate manganese sulfide. The presence of MnS is probably not due to the corrosion conditions. In the production of the alloy, manganese is commonly added to the melt to form the sulfur present into stable round sulfide inclusions that are less deleterious to the material's overall characteristics. A summary of the composition of the scale products on Specimen B is detailed in the Fig. 7 schematic.

An examination of the stainless steel sheathed thermocouple removed from Specimen A (see Fig. 8A) shows the heavy scale and the internally attacked sheathing. Observe that approximately half-way through the sheathing the internal grain boundary attack changes markedly in nature. At the outer portions the attack is heavy, the grain boundaries are very thick, and the grains large. Toward the inner portions, the attack is still heavy but it is concentrated in thinner boundaries around smaller grains.

In Fig. 8B the scale (at bottom of photo), the scale-metal interface and the internal attack along the grain boundaries are shown at higher magnification. To determine the location of sulfur, chromium, nickel and iron several x-ray maps for these elements were obtained over a more highly magnified area of the scale-metal interface (Fig. 9). From these maps it is seen that the scale layer nearest the remaining metal is primarily Cr_2O_3 with some chrome sulfide (Cr_xS_y) present. The internal attack is chrome sulfide in a heavily chrome-depleted iron-nickel matrix. Beyond the change in the nature of the grain boundary attack where the grain boundary deposits are thin and the grains smaller, it was determined that the deposits were chrome carbides. The thermocouple wires were only slightly oxidized. Figure 10 is a sketch showing the composition distribution in the attacked 304SS thermocouple sheath.

DISCUSSION

By far the most significant degree of corrosion occurring on each casing was the formation of the heavy oxide scale. While it is certainly true that some internal sulfidation was occurring, the oxide scaling appears to be responsible for the greater part of the deterioration of the well casings.

Examination of the thermocouple sheath showed advanced internal sulfidation and carburization as well as exterior oxidation but the twin sensing wires had only slight corrosion probably due to the protective influence of the ceramic housing. The minor attack on the wires is not going to affect the characteristics of the thermocouple. The ceramic housings normally come in lengths of one or two feet and the thermocouple wires are pushed into and through them.

Because of this, every one or two feet where adjacent ceramic tubes butt together, there is an area of sensing wires that essentially has no ceramic protection. These areas represent weak links in a chain for if the sulfidation ever extended through the stainless steel sheathing it could conceivably begin to attack the sensing wires and thus destroy the thermocouple's ability to measure temperature. Since there are places where the chrome sulfides extend nearly through to the ceramic, failure of the thermocouple wires by sulfidation is, indeed, a possibility.

The nature of the attack on Specimen A was much greater and of a different nature than that on Specimen B. The quantities of sulfur were much greater and appeared more distributed throughout the cross section. There must have been a greater concentration of sulfur gases in the area surrounding Specimen A.

The sulfidation of Specimen B occurred only at the edge of the base metal. Sulfur would diffuse through a slowly thickening iron oxide layer to penetrate a receding base metal layer. The brittle oxide scales, unable to keep in contact with the receding base metal, separated and formed porous layers. It is unusual to have layers of Fe_2O_3 that are as thick as those observed on Specimen B. Because of spalling and chipping of the scale during transport and mounting, there are actually many more layers of scale than those that were metallographically examined.

SIMULATED IN-SITU RETORT TESTS

Type of Shale

The retorting of different types of shale having major differences in sulfur content causes markedly different levels of corrosion to occur. Figure 11 shows cross sections of a very corrosion resistant, 310 stainless steel after similar but not exact exposures in the 10 ton simulated retort at the Laramie Energy Technology Center (LETC). Exposure temperatures were in the 925° - 1000°C max range for exposure times above 825°C of approximately 40 hours. A typical sulfur analysis of Antrim Shale shows its concentration to be 3.17 wt.%S. The sulfur analysis for a typical Green River shale only shows 0.78 wt%S.

The scale formed on the 310SS in the Antrim Shale run is much thicker than that formed in the Green River shale run. In the Antrim Shale run, the 310SS underwent internal sulfidation, forming chrome sulfides in the grain boundaries. It had a thin, broken Cr_2O_3 layer at the scale-metal interface and an external scale that was primarily a chrome sulfide near the scale metal interface and gradually became a chrome iron sulfide spinel near its outer surface (2).

The scale formed on the steel in the Green River retorting operation was a thin, continuous Cr_2O_3 with some evidence of sulfur in it. The relatively mild attack on the 310SS in this type of shale indicates it to be a promising material for thermocouple sheaths.

Type of Stainless Steel

The type of stainless steel exposed to oil shale retorting environments has a great effect on the resulting amount of corrosion. Figure 12 shows the amount and type of corrosion that occurred on type 316 austenitic stainless steel and type 410 ferritic stainless steel. The difference in chromium content, 18% for the 316SS and 12% for the 410SS was a major factor in the difference in corrosion, but not the only one. Other differences such as the crystallographic structure and the presence of nickel and molybdenum in the 316SS had their effects but it is not known how they helped to cause the considerably less severe attack on the 316SS. In coal gasification atmospheres containing both oxygen and sulfur, ferritic chrome stainless steels (446SS) behaved comparably to 300 series stainless steels (3).

Both steels were exposed in the Lawrence Livermore Laboratory (LLL) L-2 large simulated in-situ retort operating on air and saturated steam. The temperatures in this run spiked much more than in the LETC 10 retort reaching 900°C max and exceeding 825°C for only 5 hours. Green River shale was retorted. The multilayer, porous scale that formed on the 410SS is typical of heavy scale formations on any alloy in an oil shale retorting environment. It is composed of a gradation of chrome sulfides to iron-chrome sulfide spinels. The thin, primarily Cr_2O_3, scale on the 316SS should be compared to the 410's scale considering the great differences in magnification of the two pictures.

Effect of Retorting Temperature

Corrosion is a chemical reaction and is affected by temperature. Figure 13 shows the amount of scale formed on 1018 mild steel placed in two different locations in the 10 ton retort at LETC, test S-60. The test was conducted with Green River shale and air and saturated steam with a total retorting time of 64 hours, 50 hours on air and steam. The amount of scale formed at 600° and 875°C areas of the retort is markedly different; note the difference in magnification of the pictures. This test indicates that A53 mild steel piping does have a limited but possibly acceptable life at temperatures no more than 550 - 650°C in retorts. The scaling rate at the lower temperatures could be planned for.

Figure 14 shows two 310SS specimen cross sections exposed to the same two temperatures in the same retort test. It can be seen that the 310SS was below its threshold corrosion temperature for the test duration at both temperatures. Figure 14 shows the great improvement in corrosion resistance provided by stainless steel in retorting environments. However, proper material selection would indicate 1018 to be used at the lower of the two test temperatures.

Lean and Rich Shale

Oil shales vary in their organic kerogen content. Specimens were placed in the large LLL retort in run L-3. In this run both rich and lean oil content shales were tested, one in the upper part of the retort, the other in the lower part. Test specimens were placed in both sections and underwent comparable exposure

conditions. Figure 15 shows the resulting scale cross sections on 1018 mild steel specimens. The increased amount of scale formation on the specimen in the rich shale section is remarkable considering that the test conditions were comparable and both upper and lower parts of the retort had low sulfur Green River shale in them. Figure 16 shows the same comparison of 410SS; only in this case the magnification of both pictures are the same.

It is not known why such a great difference in corrosion occurred. Table 1 (4) shows the variation in sulfur content for shales with different oil contents. While the total sulfur increases with increasing oil content, its increase in the 25-50 gallon/ton range of the LLL tests does not appear to be great enough to cause the difference in scale formation. In some informally reported data on the run by LLL, their measurement of the sulfur content of the gases for the lean shale exceeded that for the rich shale. Clarification of the differences in corrosion is needed. However, the corrosion potential difference of Green River shales of varying kerogen content has been demonstrated.

PROTECTIVE COATING SYSTEMS

The relatively short time, single cycle life of metallic components in an in-situ retort makes the consideration of protective aluminide coatings attractive. The successful use of such coatings could markedly reduce the cost of reliable piping material systems that could utilize mile steel as the principal metal. Figure 17 shows two mild steel specimens, one uncoated and one coated, that were exposed in the LLL L-2 retort run. It can be seen that the presence of the high aluminum content, diffused coating on the surface of the steel maintained the original surface of the mild steel very well. The apparent pores in the outer layer of the coating are the result of alumina concentrations being pulled out in the polishing operation. Figure 18 shows a cross section where the alumina concentrations were not removed during specimen preparation.

The EDAX analyses in Fig. 18 shows that some small amount of sulfur may have diffused into the aluminum rich coating location, but did not form a deleterious sulfide. The alumina concentrates are identified by the high aluminum peak at location 2. The integrity of the surface region on the protected specimen is a marked improvement over the attack that occurs on the uncoated 1018 material. Considerable additional work is now underway to better define the role of coatings on oil shale retorting materials.

CONCLUSIONS

1. The severity of the operating conditions in actual underground in-situ oil shale retorts can exceed that which occurs in above ground, simulated retorts because of the higher temperatures which occur in the naturally insulated retorts. The result is the potential of catastrophic corrosion as occurred on the thermowell that was analyzed.

2. The selection of materials for in-situ retorts must be based on their local environmental conditions and not on an overall definition of the type of corrosive environment which occurs in a retort. Temperature, type of shale, shale oil content and other specific service conditions for the metals can cause large differences in corrosion behavior.

3. The potential of aluminide and other types of coating systems on mild steel to extend its limit of service is great and the use of coatings should be considered for mild steel and also stainless steel to extend its limits in thermocouple sheath service.

ACKNOWLEDGEMENT

This work was supported by the Office of Advanced Research and Technology, Office of Fossil Energy, U.S. Department of Energy under Contract No. W-7405-ENG-48.

REFERENCES

1. Levy, A. and Elliott, E., "Corrosion of Metals in In-Situ Oil Shale Retorts," NACE Corrosion 80, Paper No. 209, March 1980.
2. A. O. Shaeffer, Editor, "A Program to Discover Materials for the Gasification of Coal and Other Solid Fuels," Quarterly Progress Report for the period April 1, 1980 to June 30, 1980, MPC June 1980.
3. Elliott, E., "Elevated Temperature Corrosion of Oil Shale Retort Component Materials," LBL-8639, October 1978.
4. Cameron Engineering Handbook on Oil Shale and Coal.

FIGURE CAPTIONS

1. As received appearance of well casings.
2. Optical micrographs of Specimen B.
3. Optical micrographs of thermocouple.
4. Electron micrograph of Specimen B.
5. Internal sulfidation of Specimen B.
6. Internal attack in base metal.
7. Schematic of Specimen B showing various corrosion products.
8. Electron micrograph of thermocouple sheath.
9. X-ray maps of boundary layer and internal attack of sheath.
10. Schematic of thermocouple sheath showing the various corrosion products.
11. Scale X section on 310SS from Antrim and Green River shales.
12. Scale X section of 316SS and 410SS in LLL 2 retort run.
13. Scale X sections of 1018 mild steel at 600° and 875°C.
14. Scale X sections of 310SS mild steel at 600° and 875°C.
15. Scale X sections of 1018 for rich and lean shale.
16. Scale X sections of 410SS for rich and lean shale.
17. 1018 mild steel with and without aluminide coating.
18. 1018 mild steel X section of aluminide coating.

Table 1
Distribution of Sulfur in Colorado Oil Shale

							Average
Oil yield of shale, gal/ton	10.5	26.7	36.3	57.1	61.8	75.0	
Total sulfur in raw shale, percent	.62	.56	.73	1.96	1.99	1.86	
Distribution of total sulfur into types, percent:							
Organic Sulfur	27	27	37	19	21	24	26
Pyritic Sulfur	71	73	63	79	77	72	72
Sulfate Sulfur	2	trace	trace	2	2	4	2
TOTAL	100	100	100	100	100	100	100
Distribution of total sulfur in assay products, percent:							
Oil	5	11	8	7	9	11	8
Gas	2	10	19	18	23	6	13
Spent Shale	93	79	73	75	68	83	79
TOTAL	100	100	100	100	100	100	100

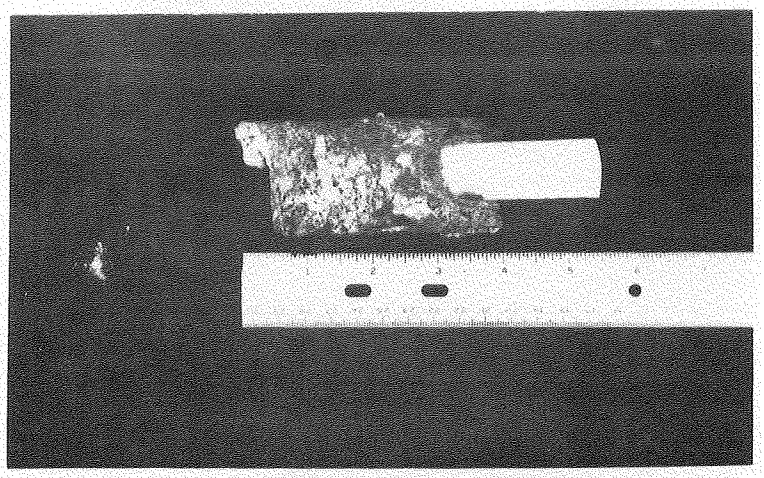

SPECIMEN A

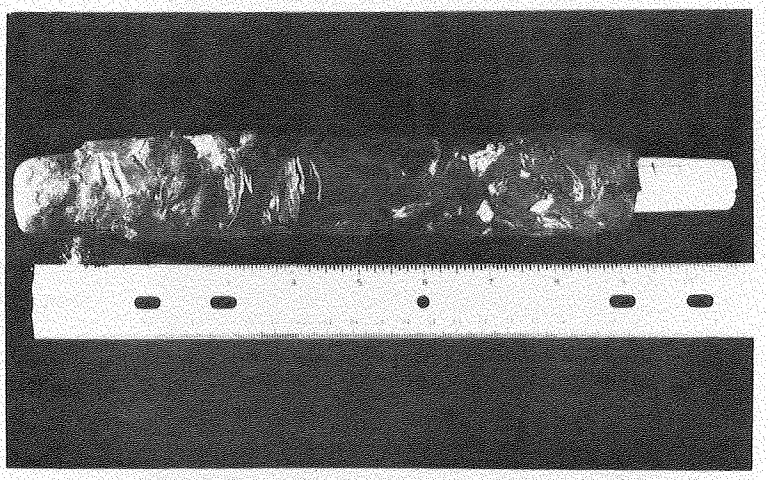

XBB 795-7101

SPECIMEN B

FIGURE 1. Initial appearance of well casings.

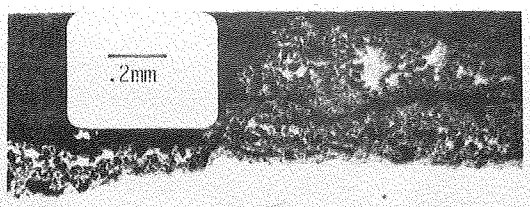

Outer Edge

2A

Inside Edge

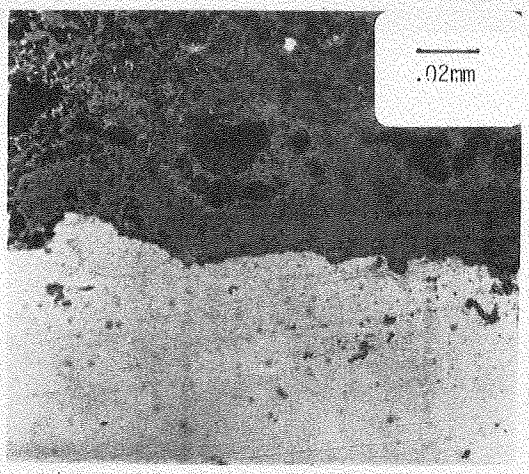

Outer Scale

2B

Base Metal

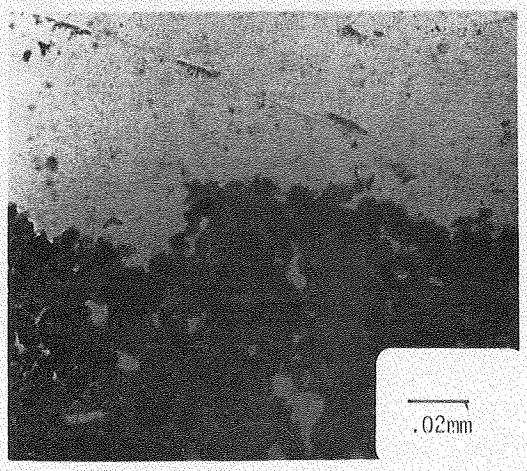

Base Metal

2C

Inner Scale

XBB 795-7091

Fig. 2 Optical micrographs of Specimen B.

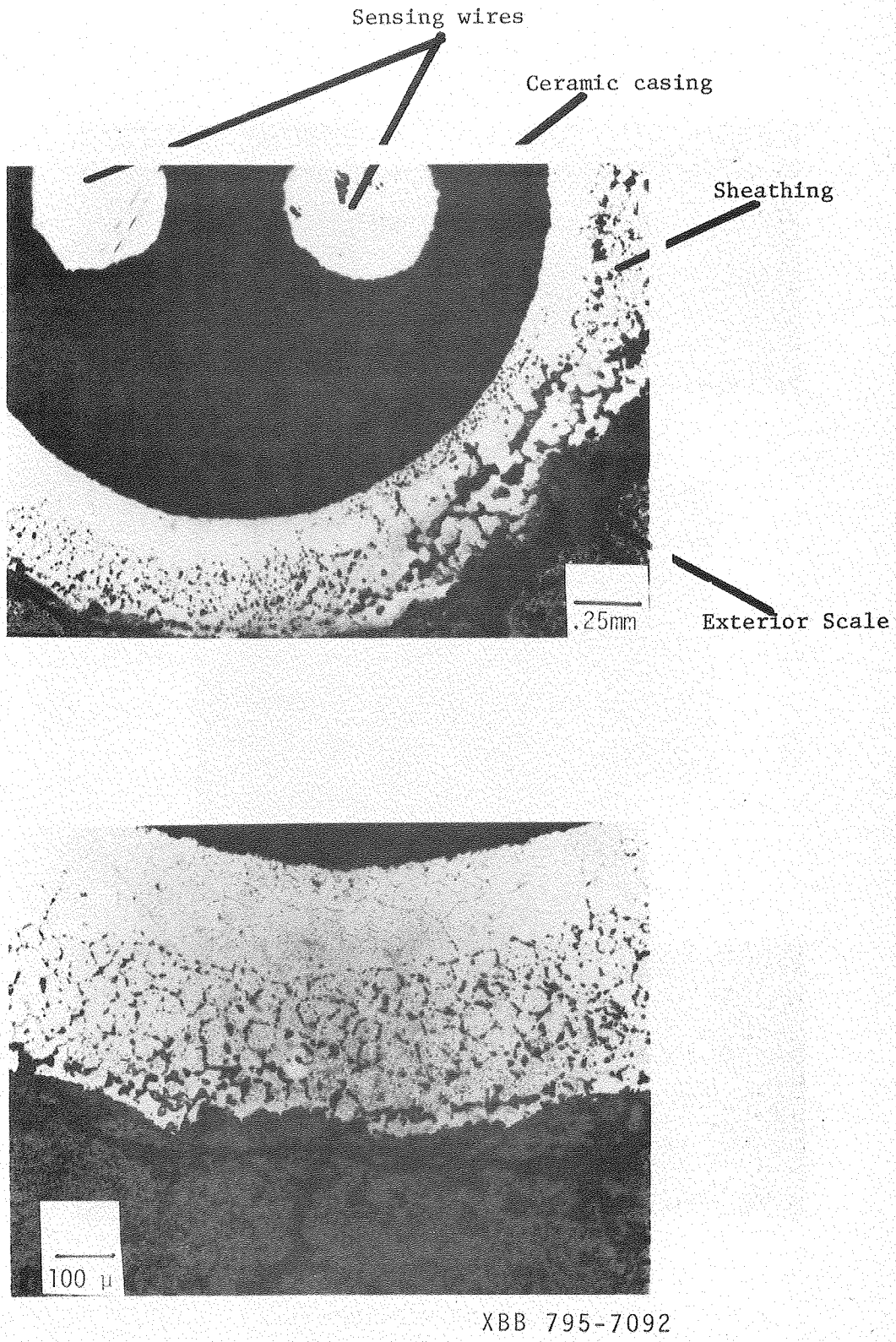

FIGURE 3. Optical micrographs of thermocouple.

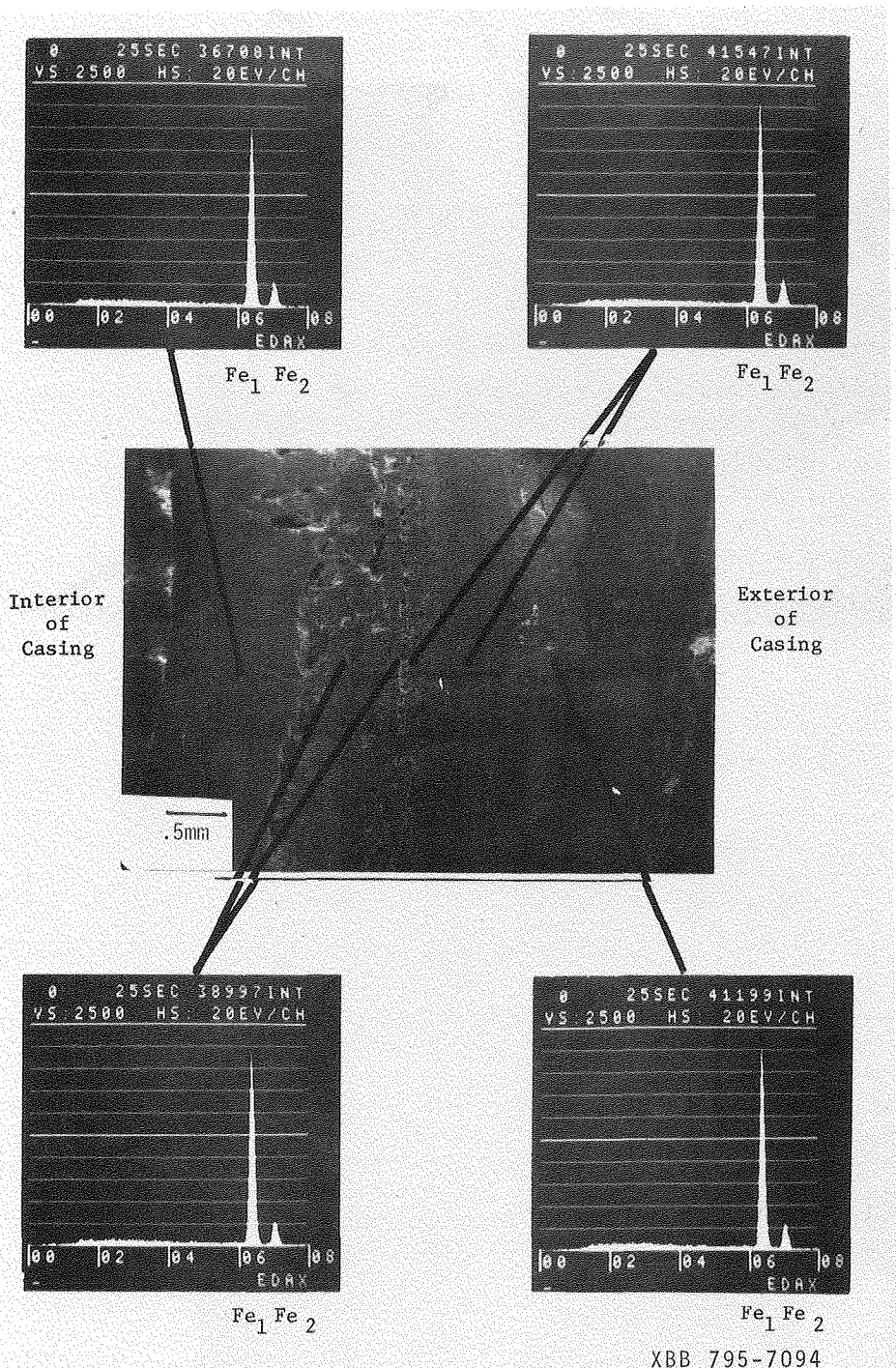

FIGURE 4. Electron micrograph of Specimen B.

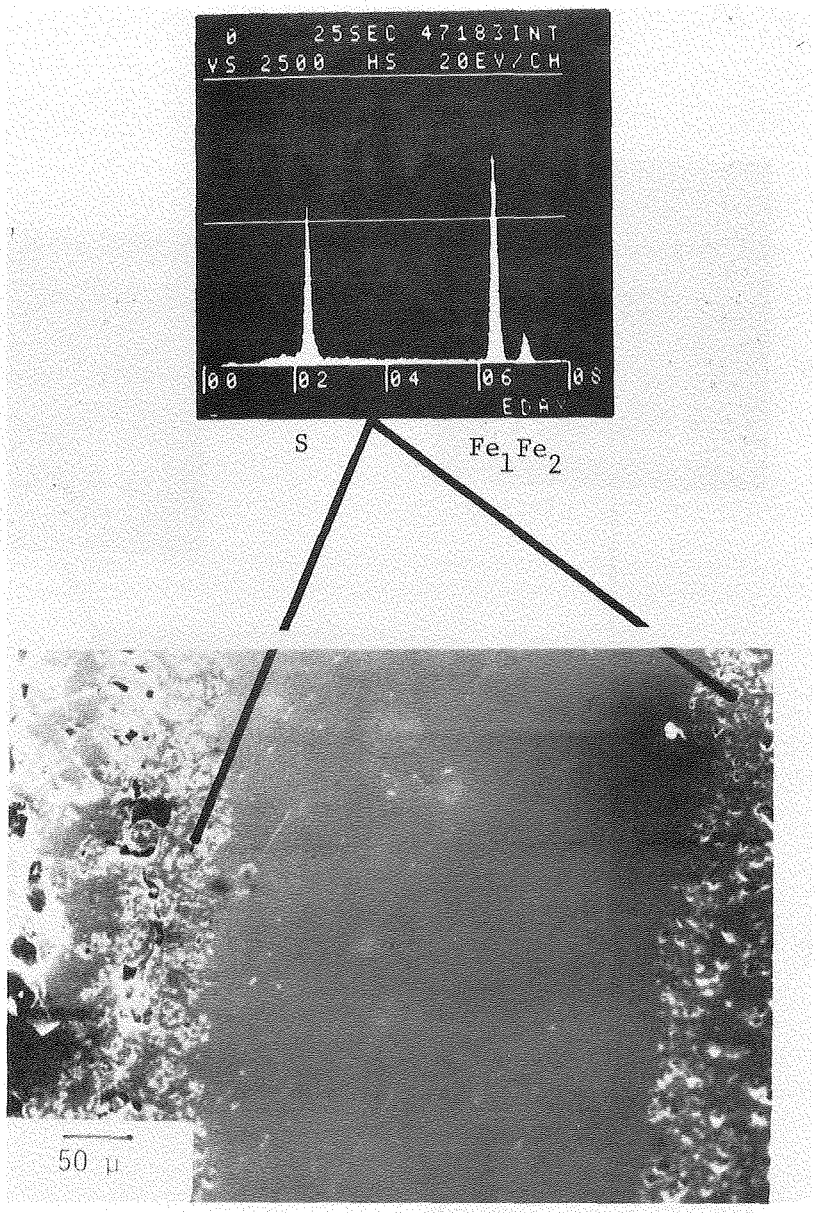

FIGURE 5. Internal sulfidation of Specimen B.

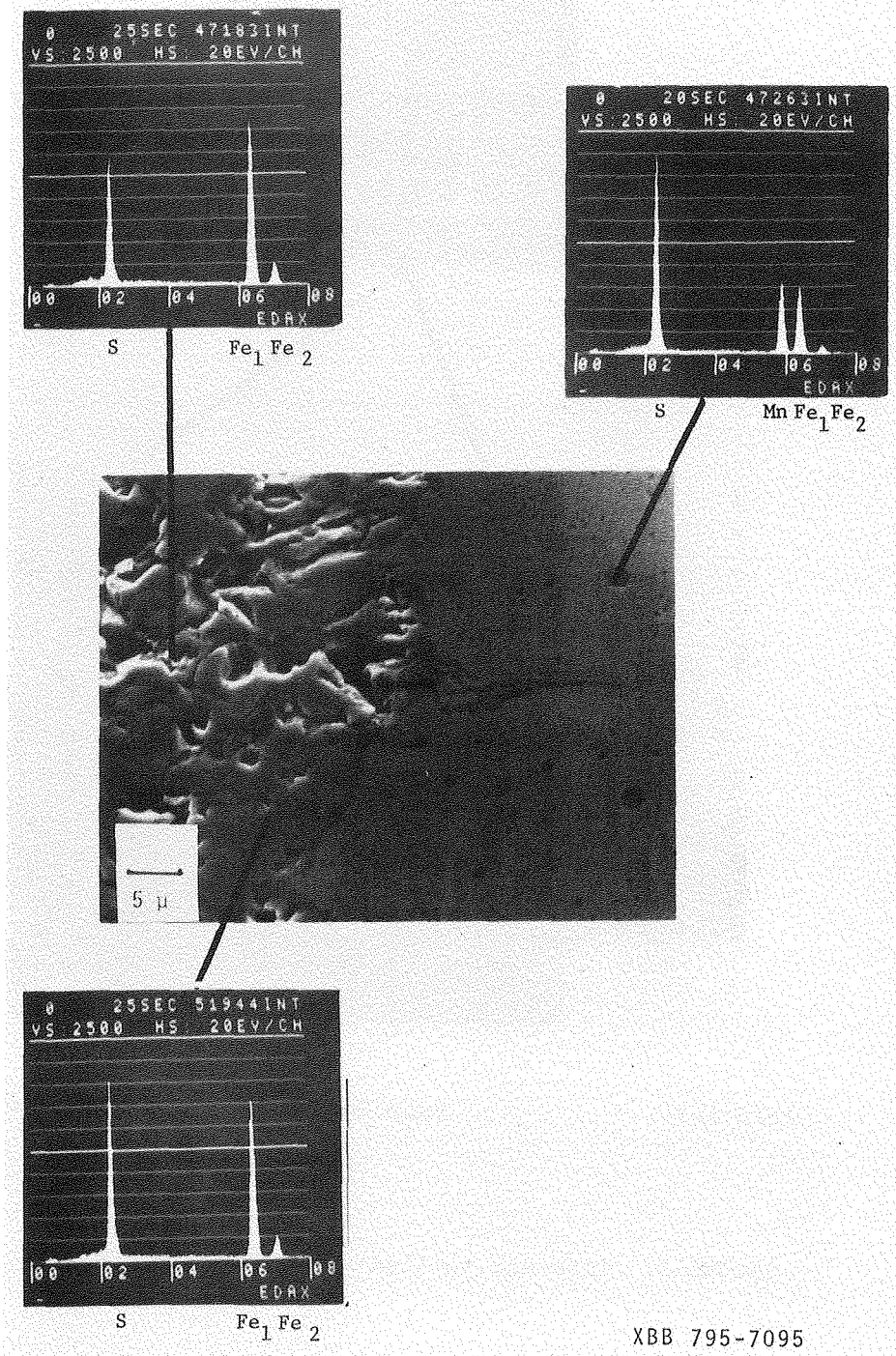

FIGURE 6. Internal attack in base metal (Specimen B).

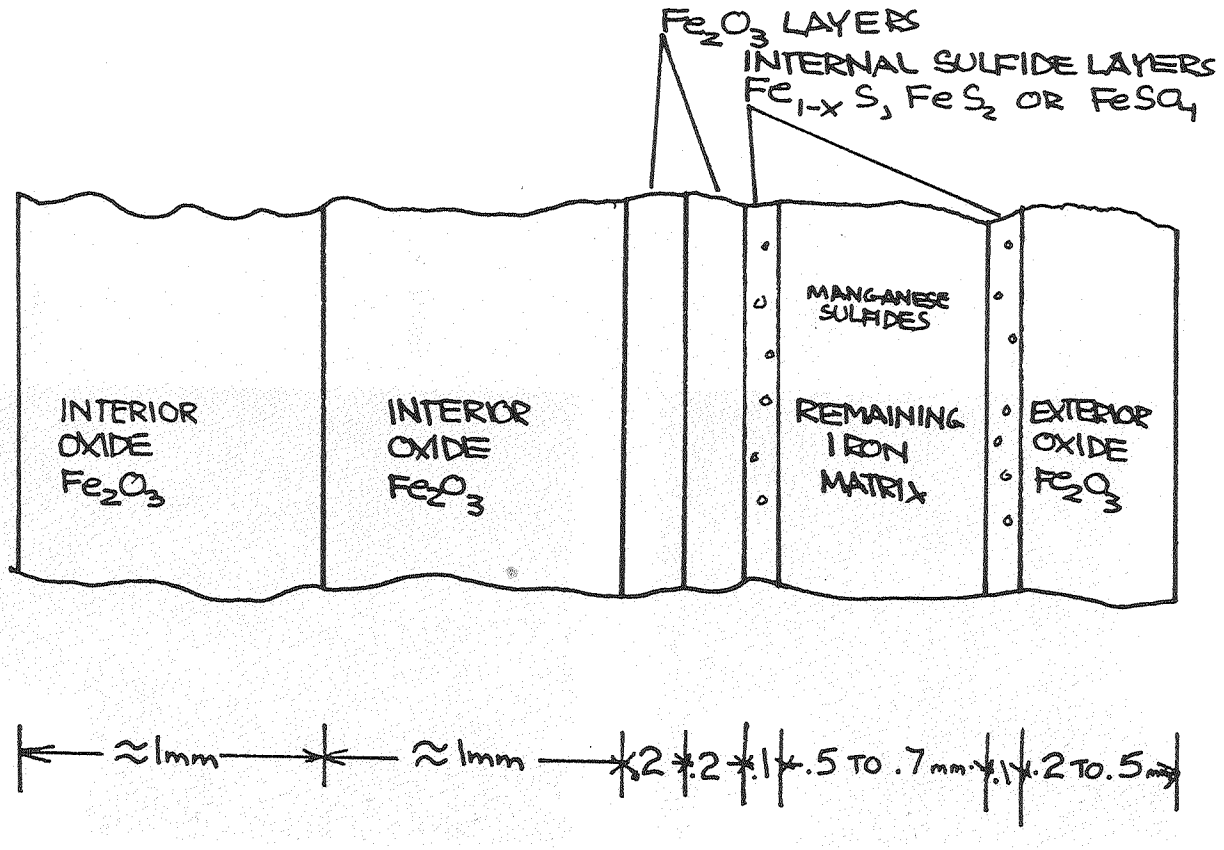

Fig. 7 Schematic of specimen B showing various corrosion products.

XBL 801-7712

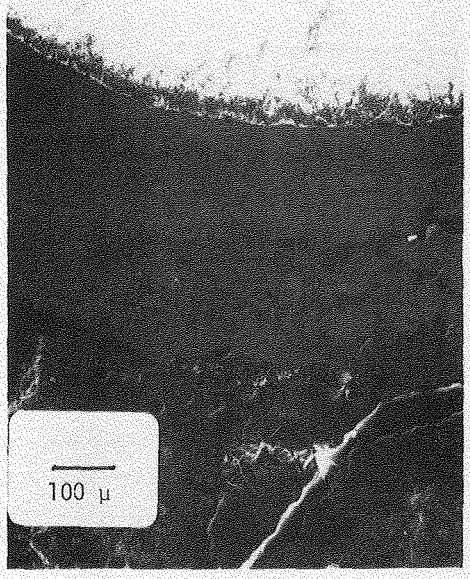

8A

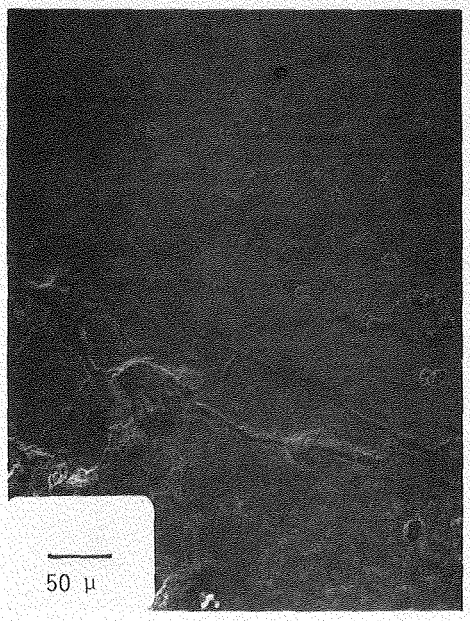

Fig. 8 8B XBB 795-7093

Electron micrograph of thermocouple sheath.

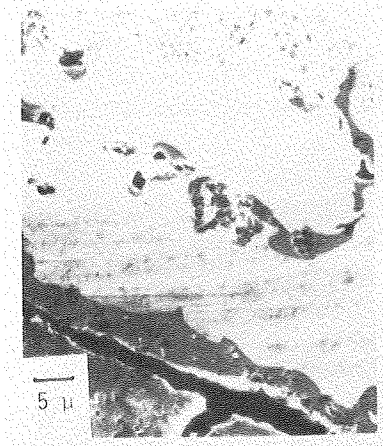

Orientation photo

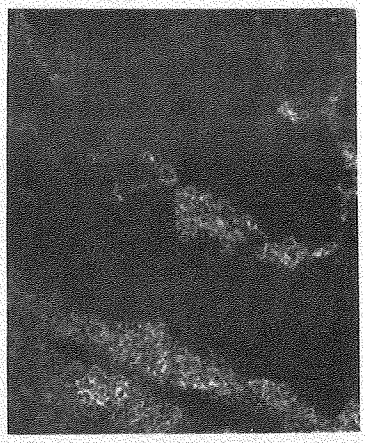

Chrome

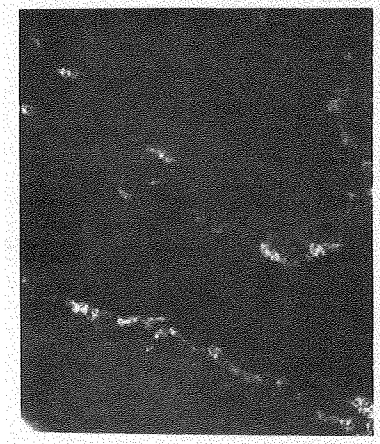

Sulfur

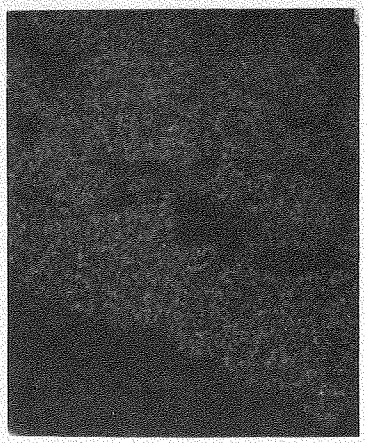

Nickel

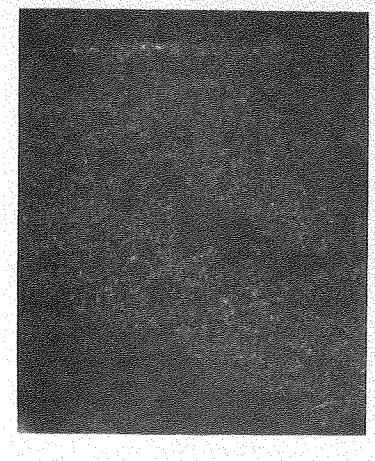

FIGURE 9. X-ray maps of boundary layer and internal attack of sheath.

XBB 795-7099

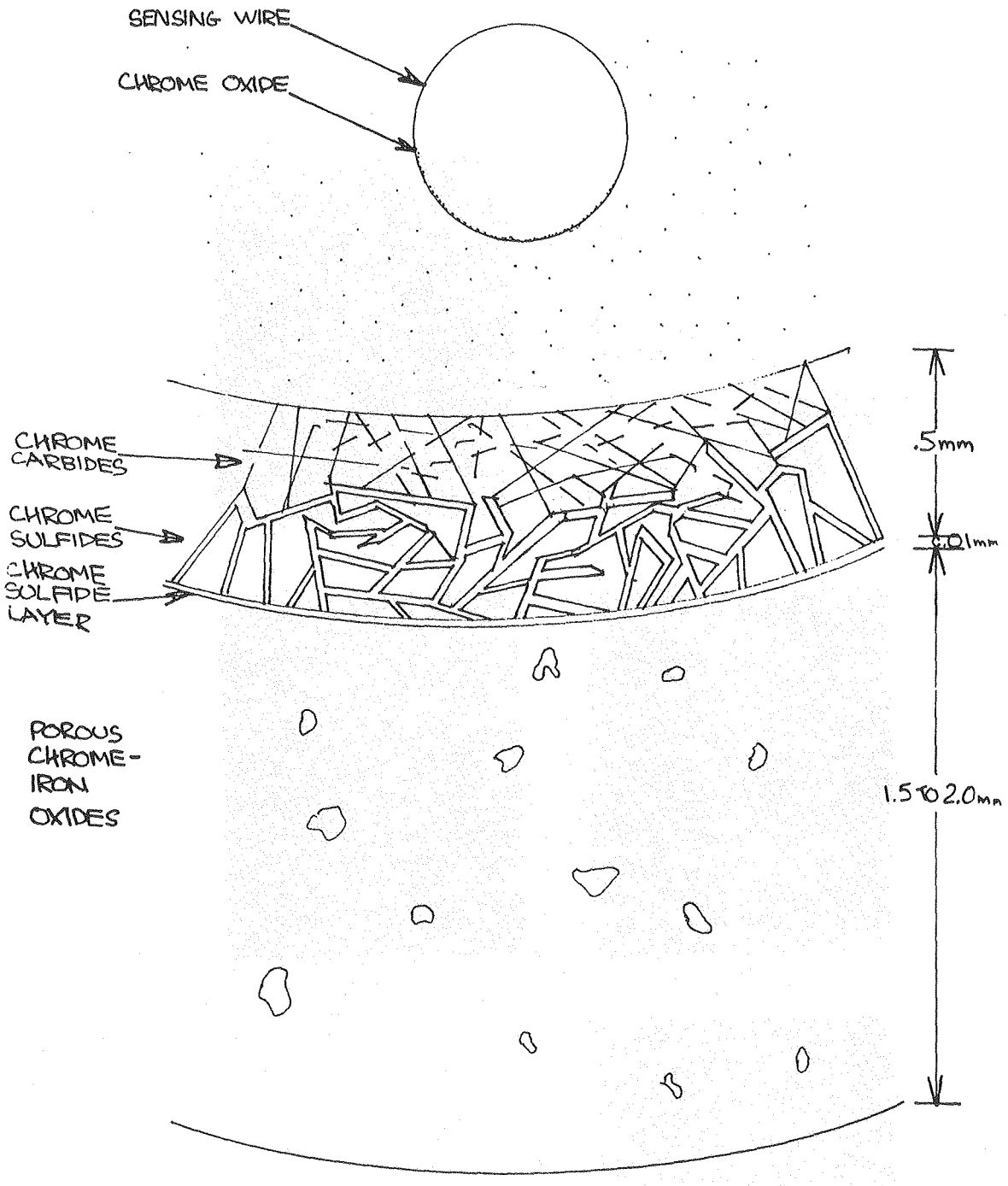

Fig. 10 Schematic of thermocouple sheath showing the various corrosion products. XBL 801-7711

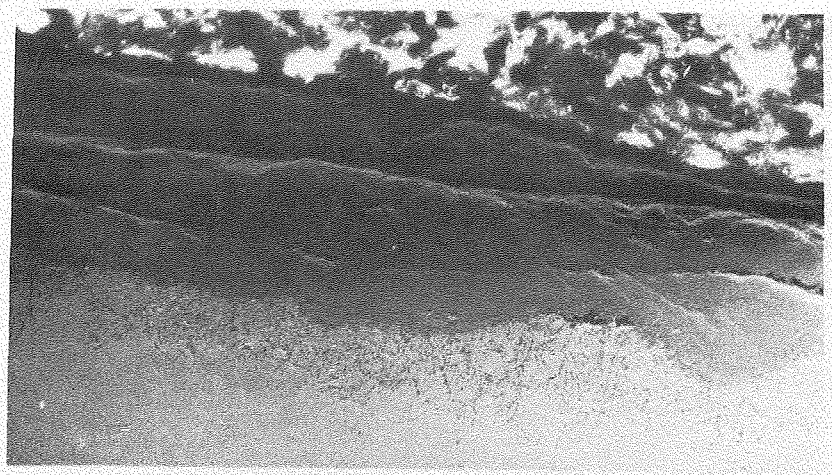

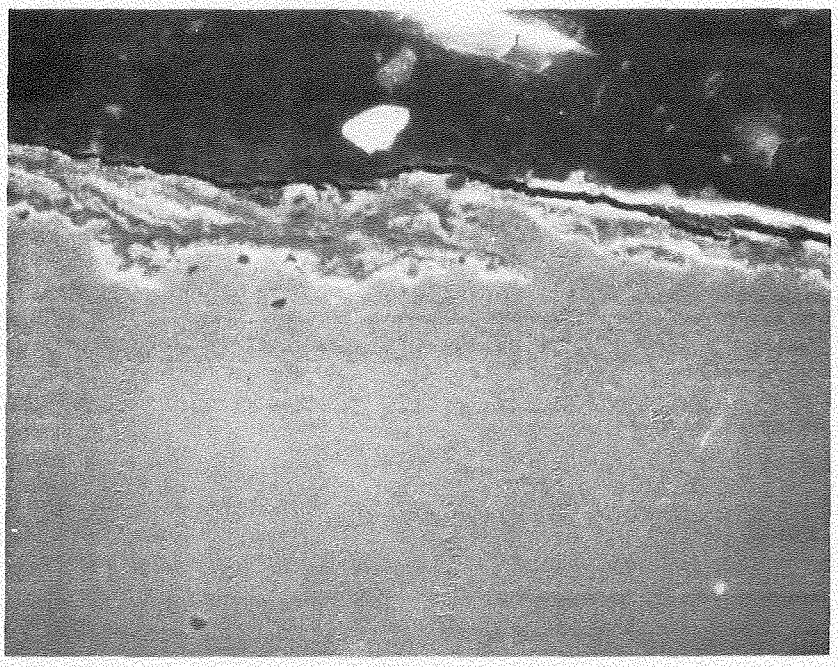

XBB 7912-16283

Fig. 11 Scale X section on 310SS from Antrim and Green River shales.

25μ

316SS

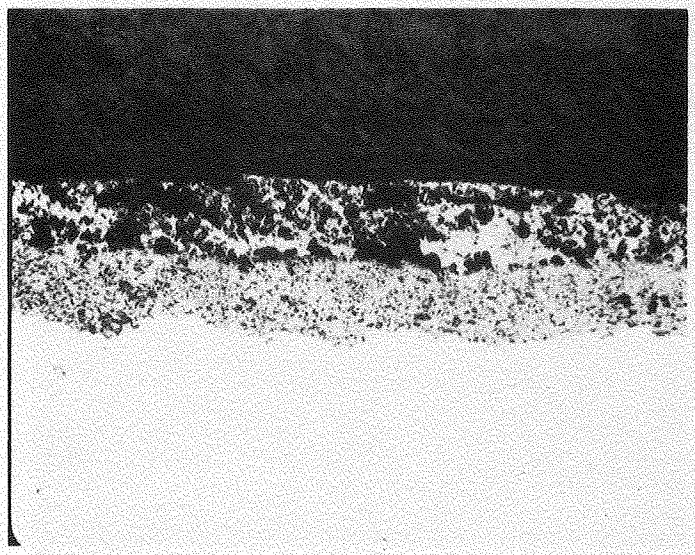

100μ

410SS

XBB 801-159

LLL
RUN 2

Fig. 12

Scale X section of 316SS and 410SS in LLL 2 retort run.

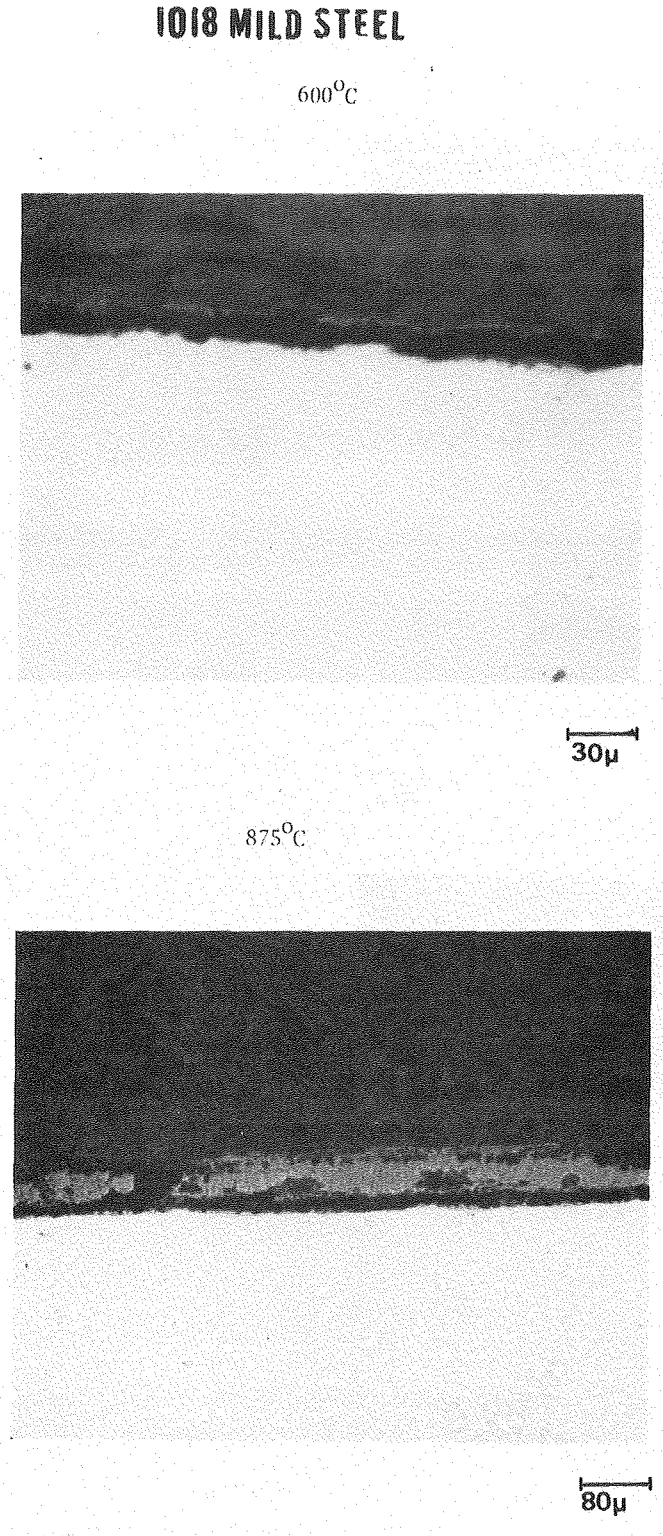

Fig. 13 XBB 810-157A

Scale X sections of 1018 mild steel at 600° and 875°C.

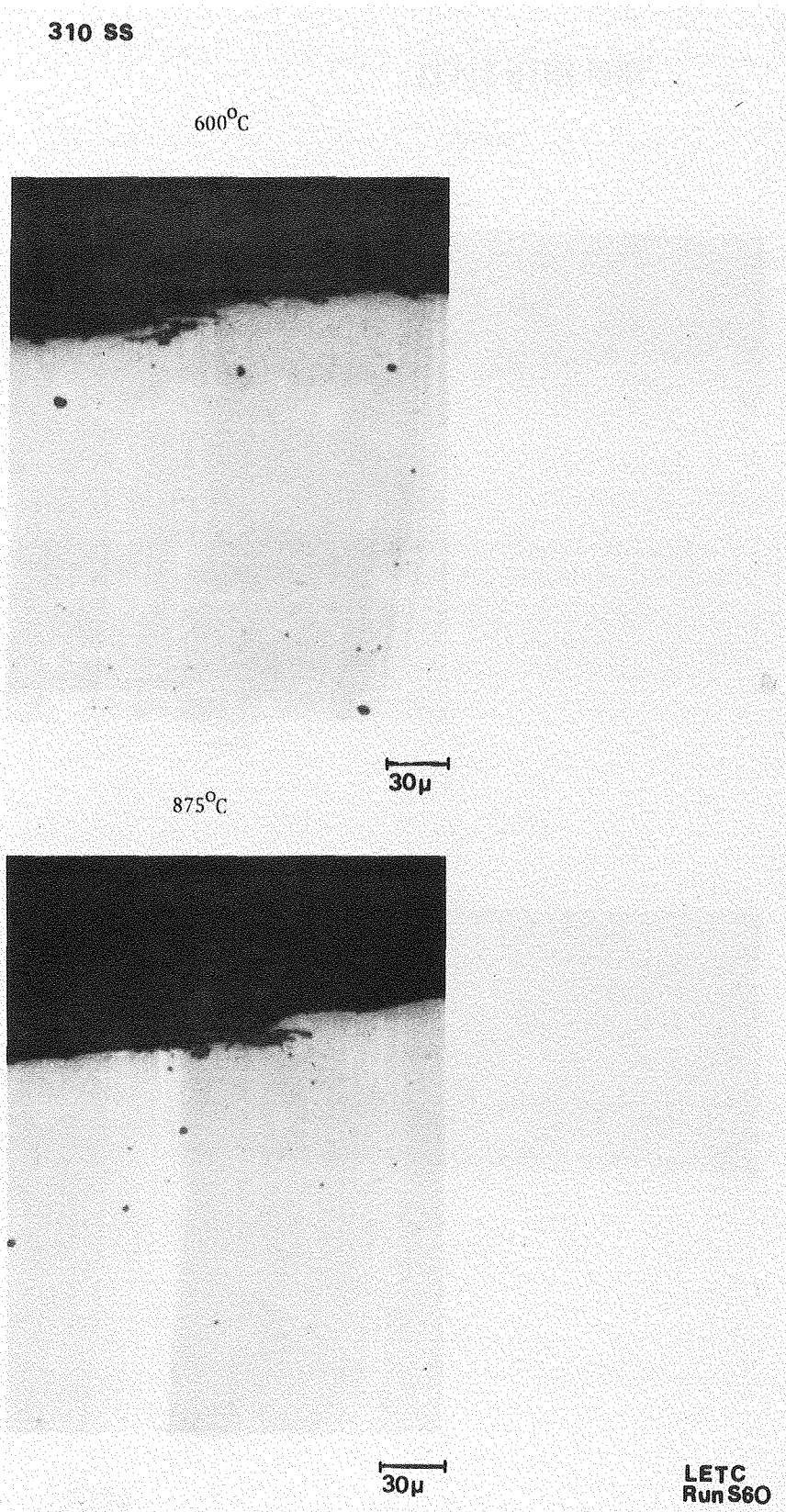

Fig. 14 XBB 801-158

Scale X sections of 310SS mild steel at 600° and 875°C.

1018 MILD STEEL

RICH SHALE

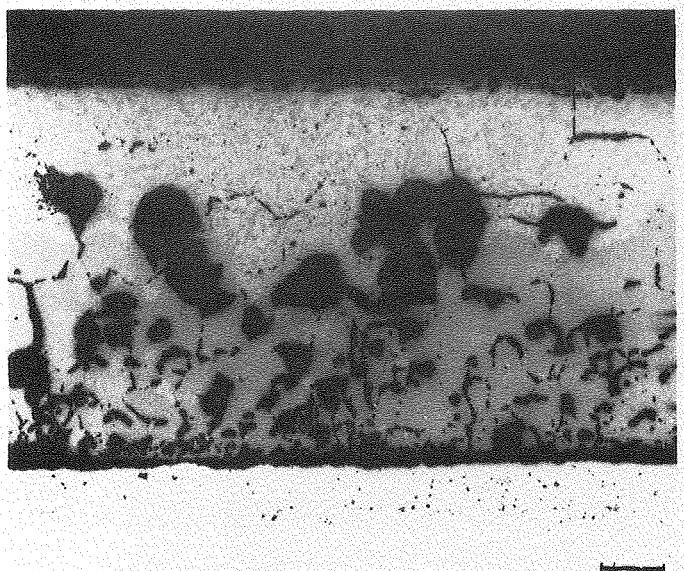

LEAN SHALE

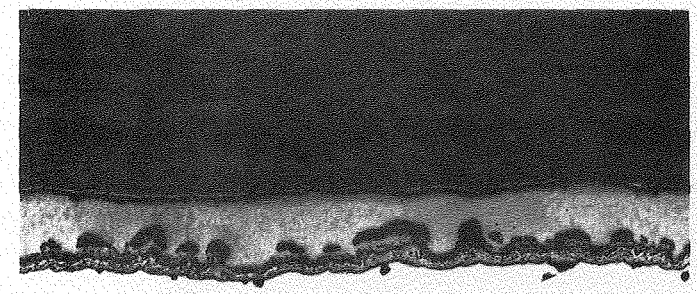

XBB 801-156

L L L
Run 3

Fig. 15
Scale X sections of 1018 for rich and lean shale.

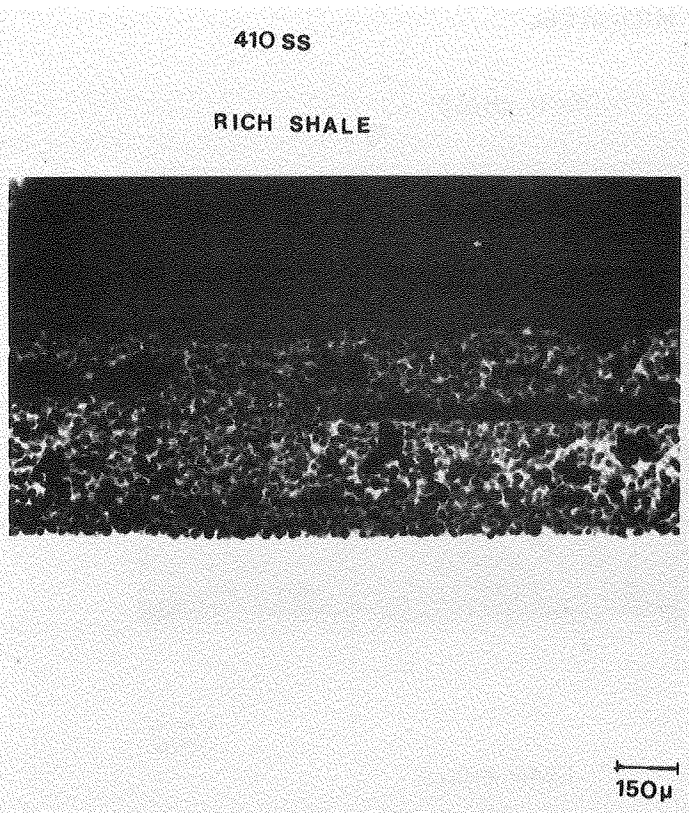

Fig. 16 XBB 801-155

Scale X sections of 410SS for rich and lean shale.

TWO 1018 S SAMPLES IN THE SAME RUN

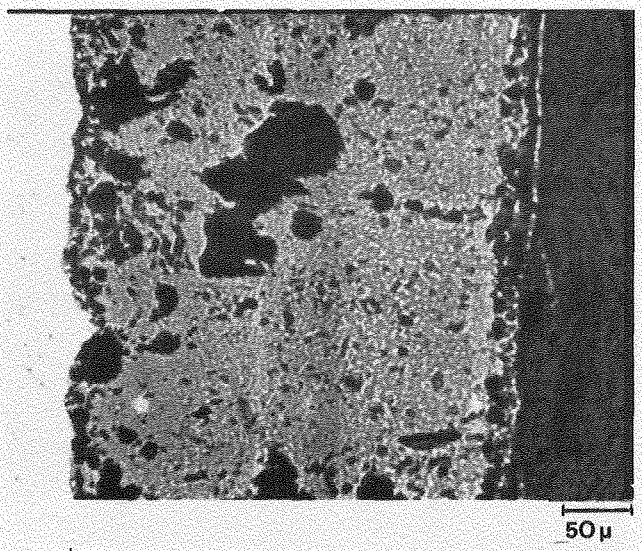

WITHOUT COATING

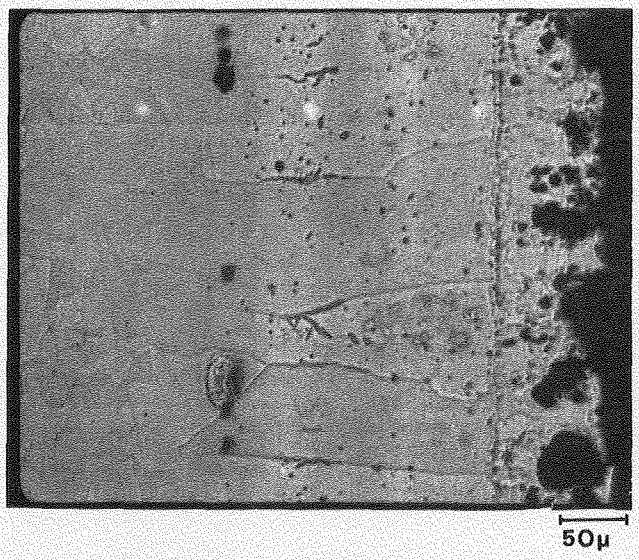

WITH COATING

Fig. 17 XBB 7912-16285
1018 mild steel with and without aluminide coating.

1018 ALONIZED STEEL

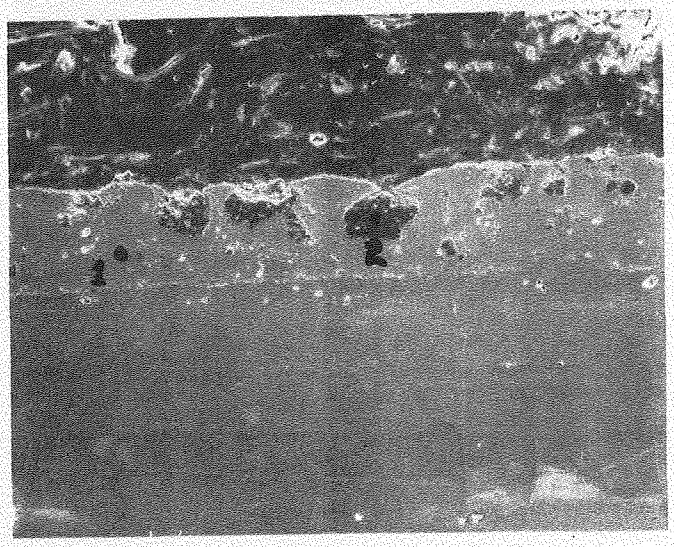

60 μ

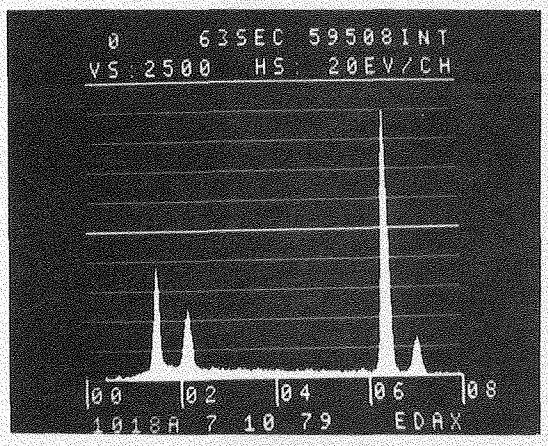

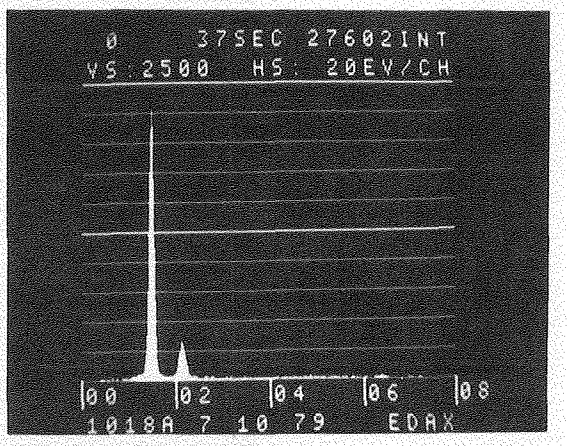

1 2

Fig. 18 1018 mild steel X section of aluminide coating.

XBB 801-160

LLL
Run 2